

## The Application of Electrodeposited Poly(Propylene imine) Dendrimer as an Immobilisation Layer in a Simple Electrochemical DNA Biosensor

Omotayo A. Arotiba<sup>1,\*</sup>, Priscilla G. Baker<sup>2</sup>, Bhekile B. Mamba<sup>1</sup>, Emmanuel I. Iwuoha<sup>2</sup>

<sup>1</sup> Department of Chemical Technology, University of Johannesburg, Doornfontein 2028, South Africa

<sup>2</sup> SensorLab, Department of Chemistry, University of the Western Cape, Bellville 7535 South Africa

\*E-mail: [oarotiba@uj.ac.za](mailto:oarotiba@uj.ac.za).

Received: 5 January 2011 / Accepted: 7 February 2011 / Published: 1 March 2011

---

We describe the application of poly(propylene imine) dendrimer in the preparation of a simple DNA biosensor. Generation one PPI was electrodeposited via cyclic voltammetry on glassy carbon electrode using a potential range of -100 to 1100 mV for 10 cycles at 50 mV/s scan rate. A single strand probe DNA (21 mer) of 2  $\mu\text{M}$  concentration was immobilised by electrostatic attraction on the PPI layer via deep coating in a 500  $\mu\text{L}$  solution for 3 hr at 25  $^{\circ}\text{C}$  to form the biosensor (GCE/G1PPI/ssDNA). Hybridisations were carried out at 38  $^{\circ}\text{C}$  using blank buffer solutions and target DNA solutions comprising of complementary, non complementary and 3 base mismatch DNA strands. Electrochemical impedance spectroscopy presented as Nyquist, impedance and phase angle plots, was used to interrogate each stage of the biosensor preparation with  $\text{Fe}(\text{CN})_6^{3-/4-}$  as the redox probe. The biosensor hybridisation performance was monitored using charge transfer resistance data obtained after fitting the impedance plot. The DNA biosensor was able to detect complementary DNA target to the limit of  $9.43 \times 10^{-12}$  M with a linear range of  $1 \times 10^{-11}$  M to  $5 \times 10^{-9}$  M. The biosensor was also selective towards mismatch and non complementary target DNA.

---

**Keywords:** biosensor, electrochemical DNA biosensor, dendrimer, poly(propylene imine) dendrimer, electrochemical impedance spectroscopy, immobilisation layer

### 1. INTRODUCTION

Electrochemical DNA biosensors (EDB) are a class of affinity sensors which can be further divided into label and label free [1-4]. The major principle of biorecognition in electrochemical DNA biosensor is based on hybridisation. The fact that hybridisation is not intrinsically an electroactive process favours the label free electrochemical DNA biosensor design. In label free approach, changes in the electrical and surface properties at the interface of the electrode are exploited. These interfacial

changes make electrochemical impedance spectroscopy (EIS) a technique of choice [5-6]. Though most of the works on EDB are still at the research level, few products can now be found in the market and some on the way. For example, Osmetech has received FDA clearance for eSensors assays for detecting cystic fibrosis carriers, and for identifying single-nucleotide polymorphisms (SNPs) as relates to warfarin. Warfarin is the most widely prescribed oral anticoagulant in North America and Europe with an estimated 2 million new patients in the US each year [7-8].

One of the philosophies of biosensor is biomimicry. Thus, biosensor development necessitates working within the biomolecular 'convenience' of the bioreceptors. This means keeping the biomolecule or bioreceptors (DNA or enzyme) in its natural (physiological) structural conformation and environment as much as possible. Thus the key step in the design of EDB is the immobilisation of the DNA probe. The success of immobilisation lies on the immobilisation layer or platform and the chemistries of immobilisation. Myriads of immobilisation layer which are usually polymeric or polymer composites [9-11] and nanomaterials [12] such as gold nanoparticle [13], carbon nanotubes [14-15], quantum dots [16] etc., have been reported. The application of these materials sometimes necessitates multiple stages of immobilisation layer preparations such as layer by layer covalent attachment via carbodimide bonds at stringent conditions. These approaches are plausible and have birthed lower detection limits, but complex protocols and chemistries may often be difficult to reproduce or produce commercially. Hence we quest for materials and approaches which are simple and DNA friendly – keeping things simple (if possible) may be a key to bigger breakthroughs and thus herald more commercially available DNA biosensors.

Dendrimers are a new class of highly branched globular polymers [17] with biocompatible properties. The dendritic architecture actually originated from nature [18] and the degree of control that exists within dendrimers and biological molecules make them a good candidate for biomimicry, hence biosensors [19]. The exploit of dendrimers in biomedical applications especially in gene delivery where it is being used as a non viral vector, is a proof of DNA-dendrimer biocompatibility [20-22].

A comprehensive report on the synthesis of the two most popular dendrimers - poly(amidoamine) (PAMAM) and poly(propylene imine) dendrimer (PPI) - have been reported by Newkome and Shreiner [23]. PPI, typical of dendrimers, is nanoscopic in size, has highly controllable molecular weight with large number of readily accessible terminal primary amine functional groups. It is cationic in nature and through its nanocavities, has the ability to host anionic molecules like DNA. Dendrimers should therefore be a material of interest in the design of EDB. The use of dendrimers, dendrimer composites and metallodendrimer in DNA biosensor and DNA microarrays is successfully emerging [24-29].

As a sequel to our earlier work on the electrodeposition and characterisation of PPI on glassy carbon electrode [30], we present the development of a label free EDB using PPI as immobilisation layer. The biosensor is developed via a simple one-step immobilisation layer synthesis and immobilisation of DNA probe. An unmodified probe ssDNA was immobilised on the PPI using electrostatic attraction and host-guest chemistry through the dendrimer nanocavities. This immobilisation approach yielded a stable biosensor with good detection limit and selectivity. Cyclic voltammetry and EIS were used as the electro-analytical tool in this work.

## 2. EXPERIMENTAL

### 2.1. Reagents and apparatus

All reagents used are of analytical grade and were purchased from Sigma Aldrich (South Africa) except stated otherwise. Ultra pure water from Millipore was used throughout the experiment. 100 mM phosphate buffer solution and 10 mM phosphate buffer saline solution (PBS) with pH 7.2 were prepared from  $\text{Na}_2\text{HPO}_4$ ,  $\text{KH}_2\text{PO}_4$  and 0.3 mM KCl (for PBS only). 5 mM (1:1) solution of  $\text{K}_3\text{Fe}(\text{CN})_6$  and  $\text{K}_4\text{Fe}(\text{CN})_6$  ( $[\text{Fe}(\text{CN})_6]^{3-/4-}$ ) was prepared in 100 mL of 10 mM PBS pH 7.2. DNA sequences of 21 mer were purchased from Inqaba biotec, Pretoria, South Africa and shown below:

Probe: 5'-GAGGAGTTGGGGGAGCACATT-3'

Complementary: 5'-AATGTGCTCCCCCAACTCCTC-3'

Non complementary: 5'-AACGTGTGAATGACCCAGTAT-3'

3 base mismatch: 5'-AATGTGGTCGCCCTACTCCTC-3'

100  $\mu\text{M}$  of DNA stock was prepared in Tris-EDTA buffer (pH 8.0) and stored at  $-20\text{ }^\circ\text{C}$ . Working DNA solutions were prepared by diluting the stock solution to the desired concentrations in phosphate buffer solution, stored at  $4\text{ }^\circ\text{C}$  and not used when older than 4 weeks. Hybridisation was done in phosphate buffer saline (PBS). Generation one G1 poly(propylene imine) dendrimer (used as received) were purchased from SyMO-Chem, Eindhoven, Netherlands.

A three electrode system was used to perform all electrochemical experiments with glassy carbon electrode (diameter 0.3 cm), Ag/AgCl (3M Cl<sup>-</sup>) and platinum wire used as working, reference and counter electrodes respectively. All solutions were de-aerated by bubbling argon through it for 5 minutes. All voltammetric experiments were performed on an Epsilon (BASi) electrochemical workstation (LaFayette) with oxidative scan direction except stated otherwise. Square wave voltammetry (SWV) measurements were performed by applying amplitude of 25 mV and frequency of 15 Hz. electrochemical impedance spectroscopy (EIS) measurements were recorded with Zahner IM6ex Germany and Autolab PGSTAT 302N, at perturbation amplitude of 10 mV within the frequency range of 100 kHz to 100 mHz.

### 2.2. Electrodeposition of G1 PPI

The method of electrodeposition and characterisation of G1PPI onto the surface of glassy carbon electrode (GCE) has been reported in our earlier work [30]. Briefly, generation one PPI was deposited onto the glassy carbon electrode from a solution of 10 mM G1PPI in 0.1 M phosphate buffer solution using cyclic voltammetry. The electrode potential was cycled from  $-100\text{ mV}$  to  $1100\text{ mV}$  for

10 cycles at 50 mV/s scan rate. The resulting modified electrode was labelled GCE/G1PPI. After electrodeposition, the GCE/G1PPI electrode was stored either at room temperature or at 4 °C.

### 2.3. Immobilisation of probe DNA, stability, hybridisation and denaturation

Immobilisation of the single strand probe DNA (or probe ssDNA) onto the GCE/G1PPI nanoelectrode was carried out by dipping a previously argon-dried GCE/G1PPI into a 500 µL solution of 2 µM probe ssDNA for 3 hr at 25 °C. Followed by successive rinsing with water and phosphate buffer solution to remove any unbound or weakly bound probe ssDNA. The biosensor was stored at 4 °C when not in use. The biosensor was characterised by voltammetry in PBS and by EIS in 5 mM  $[\text{Fe}(\text{CN})_6]^{3-/4-}$ . The biosensor was labelled GCE/G1PPI/ssDNA. For stability studies of the biosensor as a result of storage, impedance measurements of the GCE/G1PPI/ssDNA were carried out at various time intervals in the presence of  $[\text{Fe}(\text{CN})_6]^{3-/4-}$  redox probe.

Hybridisation was carried out by immersing GCE/G1PPI/ssDNA in either blank solution or in target ssDNA solutions for 45 min at 38 °C. Blank measurements were carried out in a 1 mL solution of 10 mM PBS void of DNA. For target ssDNA, a 1 mL solution of 10 mM PBS containing different concentrations of complementary ssDNA (target ssDNA) ranging from 0.01 to 5 nM was used for the hybridisation (labelled GCE/G1PPI/dsDNA). For each hybridisation step, the hybridised biosensor was washed with water and phosphate buffer solution respectively to remove unbound target ssDNA before taking measurements. The EIS responses of the biosensor to the target ssDNA were measured in PBS and  $[\text{Fe}(\text{CN})_6]^{3-/4-}$  redox probe.

For denaturation the hybridised biosensor (GCE/G1PPI/dsDNA) was immersed into a 6 M urea solution with gentle stirring for 25 minutes in total. The denatured electrode (GCE/G1PPI/den) was then characterised by EIS.

## 3. RESULTS AND DISCUSSION

### 3.1. Immobilisation of probe ssDNA

After electrodeposition of the G1 PPI, similar characterisation and results consistent with our previous report were obtained [30]. The probe ssDNA was immobilised on the GCE/G1PPI platform via physical and electrostatic adsorption. The cationic and anionic nature of PPI and DNA respectively created the electrostatic attraction. Dendrimers have been shown to encapsulate or bind effectively with DNA or gene in the biomedical field of gene and drug delivery [21]. This ability to encapsulate DNA was exploited in the immobilisation step coupled with the electrostatic force of attraction. The impedance data of the various steps in the biosensor development using  $[\text{Fe}(\text{CN})_6]^{3-/4-}$  redox probe are presented as Nyquist plot, phase angle plot and impedance plot in Fig. 1a-c respectively. All the data obtained were verified using Z-HIT plot (see supplementary data of ref [30] for a typical plot) and the observed good correlation substantiated the reliability of the impedance data [30-31]. The Z-HIT test is a mathematical equation that derives a theoretical (or calculated) impedance data from the

experimental phase angle data and then correlates this calculated impedance with experimentally obtained impedance data. It is another way of testing the reliability of impedance data apart from the more popular Kramers - Kronig check. After the electrodeposition, there was a marked reduction in the charge transfer resistance from 1865  $\Omega$  for bare GCE to 165  $\Omega$  for the GCE/G1PPI. This is because the dendrimer layer enhanced the interfacial electron transfer of the  $[\text{Fe}(\text{CN})_6]^{3-/4-}$  redox probe [30]. Electrostatic attraction between PPI (cationic) and  $[\text{Fe}(\text{CN})_6]^{3-/4-}$  (anionic) also contributed to this  $R_{ct}$  decrease.

Impedance parameters such as maximum frequency ( $\omega_{\max}$ ), time constant ( $\tau$ ) and  $R_{ct}$  are indicators of the interfacial kinetics of a reaction [30, 32]. The phase angle is a very sensitive impedance data and it can also be related to the kinetics of a reaction using equation 1 and 2. If we take the frequency at which we have the maximum phase angle as  $f_\phi$ , and rewrite  $\omega_{\max}$  as  $\omega_\phi$  (from  $\omega = 2\pi f$ ), equation 1 shows how phase angle relates the charge transfer resistance denoted as  $R$  in the equation. Equation 2 also relates the phase angle to charge transfer resistance. Thus equations 1 and 2 [33] show that  $f_\phi$  is inversely proportional to  $R_{ct}$  and phase angle ( $\phi$ ) is directly proportional to  $R_{ct}$  respectively. These equations explain what we observed at each stage of the biosensor development. Thus, the phase angle plot can be used to monitor various stages of electrode modifications aside the commonly used Nyquist plot. After electrodeposition,  $f_\phi$  shifted to a higher frequency and the phase angle decreased (Fig. 1b and table 1). Our data thus validates this equation. A similar trend is seen in the impedance plot (Fig. 1c). More detailed discussions on the electrodeposition have been reported [30].

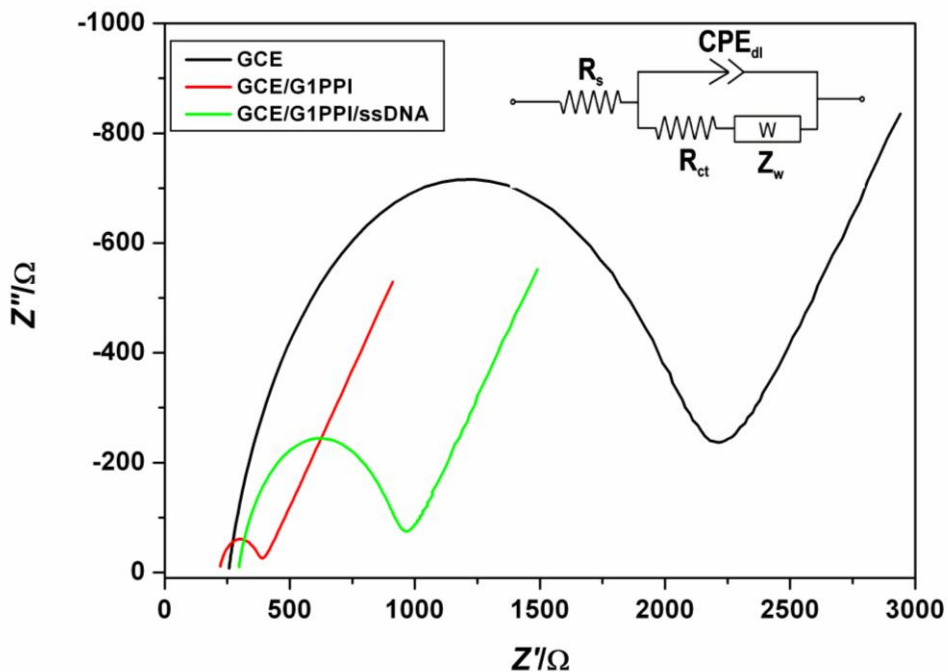
As regards the immobilisation of the 2  $\mu\text{M}$  probe ssDNA, charge transfer resistance increased by about 290% in the presence  $[\text{Fe}(\text{CN})_6]^{3-/4-}$  redox probe (Fig. 1a). The  $R_{ct}$  increased after immobilisation because of the repulsion between the anionic ssDNA and anionic  $[\text{Fe}(\text{CN})_6]^{3-/4-}$  which hinders the flow of charge or ion onto the platform [25-27, 34-35]. The presence of ssDNA slows down the interfacial electron kinetics of the  $[\text{Fe}(\text{CN})_6]^{3-/4-}$ . This phenomenon also resulted in the decrease in  $f_\phi$ , the increase in phase angle (Fig. 1b and table 1) and the increase in impedance (Fig. 1c). Square wave voltammogram (Fig. 1d) after immobilisation, also showed reduced cathodic and anodic peak currents of the PPI in PBS. This peak reduction resulted from the poor conductivity of ssDNA which deterred the flow of charged into the PPI matrix. The reduced peak currents are observed in EIS as increased  $R_{ct}$ .

The impedance parameters in table 1 were obtained from the fitting of the data in Fig. 1a and b using the common Randles equivalent circuit (Fig. 1a inset). The biosensor was stored with the surface moist at 4  $^\circ\text{C}$ . There was only about 10% reduction in the  $R_{ct}$  signal of the GCE/PPI/ssDNA upon storage for 2 months depicting good sensor stability.

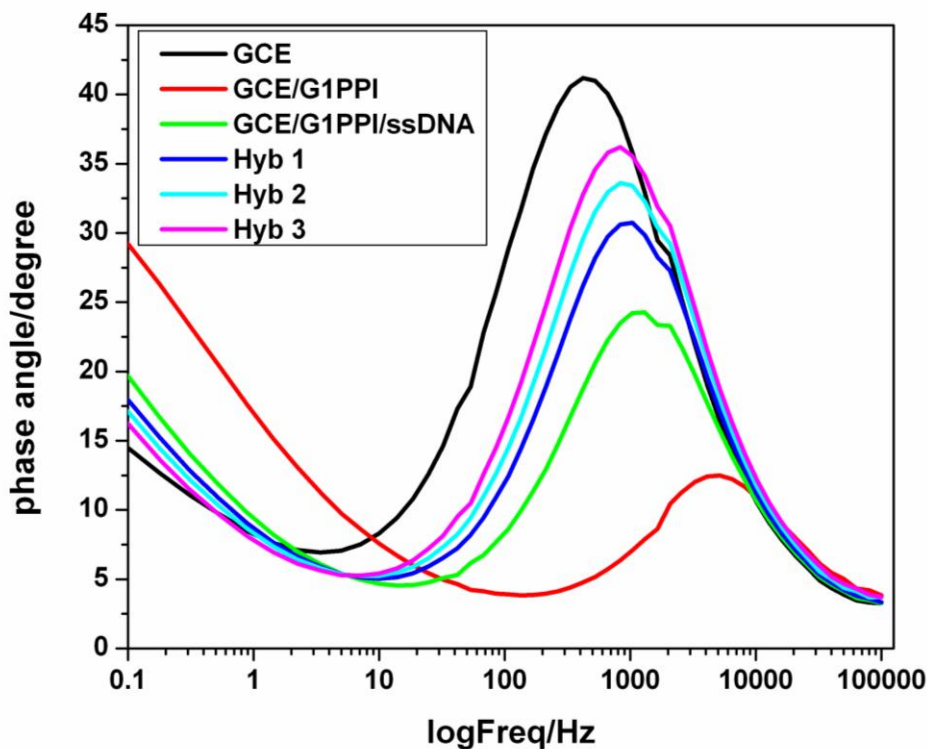
$$f_\phi = \frac{1}{4\pi RC} \sqrt{1 + \frac{R}{R_s}} \quad (1)$$

$$\phi = \tan^{-1} \left( \frac{1}{1 + 2R_s/R} \right) \quad (2)$$

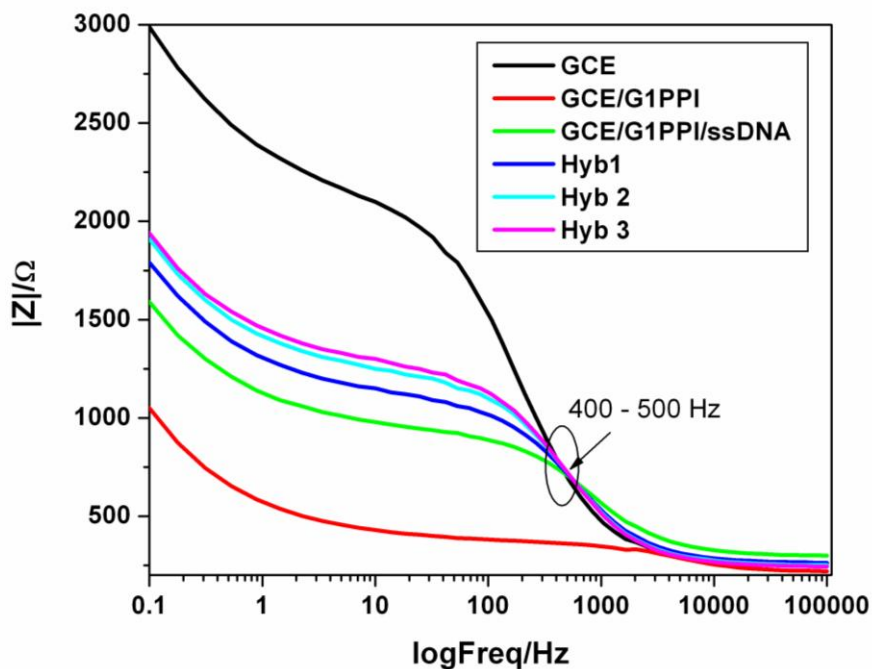
Equation (1) can be rewritten as  $\tau = \frac{1}{4\pi f_\phi} \sqrt{1 + \frac{R}{R_s}}$  or  $\tau = \frac{1}{2\omega_\phi} \sqrt{1 + \frac{R}{R_s}}$  so as to relate it to time constant  $\tau$ .



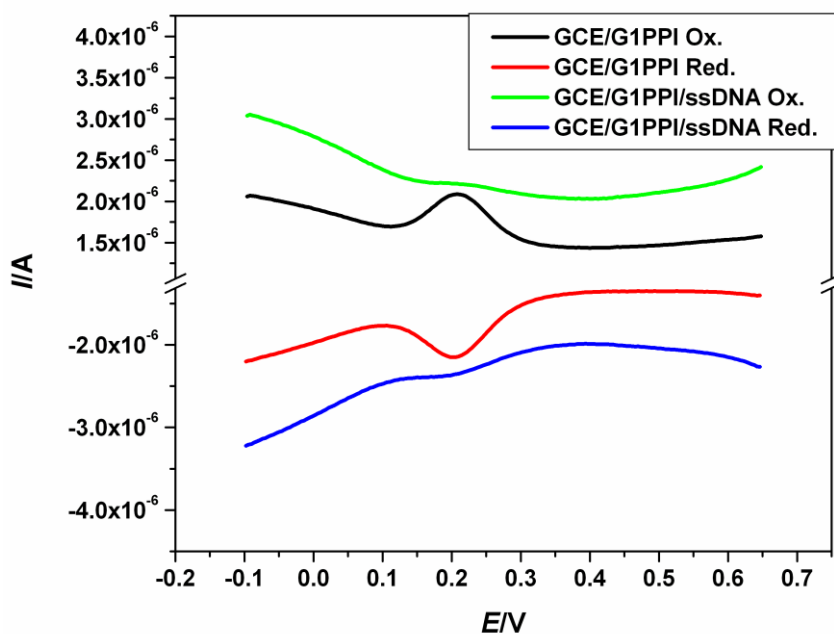
(a)



(b)



(c)



(d)

**Figure 1.** EIS plots in  $[\text{Fe}(\text{CN})_6]^{3-/4-}$  redox probe showing: (a) Nyquist plot of the bare electrode (GCE), the electrodeposited PPI (GCE/G1PPI) and the immobilised DNA probe (GCE/G1PPI/ssDNA). (b) Phase angle plot corresponding to the Nyquist but includes hybridisation with different DNA target concentration. (c) Impedance plot of the EIS data in b. (d) Anodic and cathodic square wave voltammograms in 10 mM PBS showing the effect of probe immobilisation (GCE/G1PPI/ssDNA) on the dendrimer immobilisation layer (GCE/G1PPI)

**Table 1** Electrochemical impedance spectroscopy fitting parameters obtained from Fig. 1a and b

Circuit element	GCE	GCE/G1PPI	GCE/G1PPI/ssDNA
$R_s$ ( $\Omega$ )	254.8	217	293.5
$R_{ct}$ ( $\Omega$ )	1865	165.4	643
CPE (mF)	460.7	335.3	354.6
$Z_w$ ( $k\Omega/s^{1/2}$ )	928.1	593.3	617.9
Phase shift $ \varphi $	41.2	12.9	24.3
$f_\phi$	419	5160	1189

### 3.2 Single stranded DNA target Hybridisation

Electrochemical impedance spectroscopy was used to monitor the hybridisation with  $R_{ct}$  as the analytical parameter. The average error for  $R_{ct}$  was less than 2% in all cases from the fitting results. Charge transfer resistance increased with increase in the concentration of the target ssDNA (Fig. 2). This is due to the increase in the density of the anionic charge of the DNA at the DNA/[Fe(CN) $_6$ ] $^{3-/4-}$  interface. The more the dsDNA formed as a result of hybridisation, the more the density of the anionic phosphate backbone. This increases the barrier for interfacial electron transfer of the anionic reporter (i.e. the [Fe(CN) $_6$ ] $^{3-/4-}$  redox probe) onto the electrode surface [25-26, 36]. To obtain a calibration curve (Fig. 2 inset), the  $R_{ct}$  (quadruplet measurements) was normalised by subtracting 28  $\Omega$  (the noise due to first blank measurement) from each hybridisation value and plotted against the log of concentration. A linear range of 0.01 to 5 nM and a regression equation of  $y(\Omega) = 117.04(\log x) + 2139$  with a correlation coefficient of 0.993 were obtained. The detection limit was calculated using  $3\sigma$  and a value of  $9.43 \times 10^{-12}$  M was obtained (where  $\sigma$  is the standard deviation of the blank,  $n=6$ ).

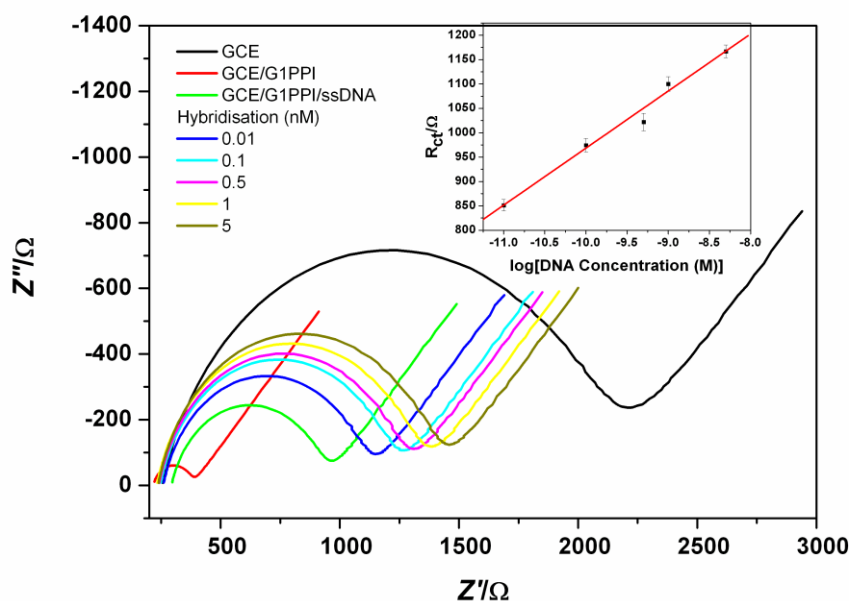


**Figure 2.** Hybridisation response of the biosensor (GCE/G1PPI/ssDNA) to target DNA concentrations. The Inset is the linear plot of normalised  $R_{ct}$  versus log of target ssDNA concentration



It is interesting to know that concentration of target DNA is also directly proportional to phase shift ( $\phi$ ) and maximum phase frequency ( $f_{\phi}$ ) as seen in Fig 1b with a correlation coefficient of 0.925 and 0.986 respectively. Also, at a chosen frequency below 400 Hz (Fig. 1c) the impedance change due to hybridisation is well resolved and hence can be used to monitor the effect of hybridisation. The phase angle plot may therefore be exploited for sensor calibration apart from the more common Nyquist plot.

### 3.3 Denaturation of the hybridised biosensor

Ideally after denaturation, the  $R_{ct}$  should return to a value very close to that of the biosensor (GCE/G1PPI/ssDNA) because denaturation is just a process of unwinding the double stranded DNA that was formed during the biorecognition event. At high pH, the hydrogen bond between the target ssDNA and probe ssDNA (the dsDNA) is broken leaving the anchored probe ssDNA on the electrode surface.

A 0.5 nM complementary ssDNA hybridised electrode was immersed in the 6 M urea solution with gentle stirring firstly for 10 minutes and then for another after 15 minutes. The measured  $R_{ct}$  after denaturation in both cases were inconsistent and both were inaccurate when compared to the expected initial  $R_{ct}$  due to probe ssDNA only.

Series of denaturation using freshly prepared biosensors also yielded inconsistent results indicating that the biosensor may be more suitable for single use. The failure to regenerate the biosensor, from the authors' perspective, is not really a disadvantage if the electrochemical DNA biosensor is seen from the view point of commercialisation and the end user.

Firstly, if saving cost is the challenge, a cheap material such as screen printed carbon electrode which can be disposed after use is envisaged and thus regeneration is not necessary. Secondly, regeneration opens door to the contamination of the biosensor.

Thirdly, regeneration takes the user back to the time consuming experimental routine and expertise, which defeats the purpose of the biosensor. Attempts to regenerate DNA biosensors may be more of academic than commercial practicability. However the GCE/G1PPI [30] and the biosensor responses to hybridisation show good reproducibility as denoted by the error bars in the calibration plot (Fig. 2).

### 3.4 Selectivity of the biosensor

The biosensor's responses to 0.5 nM concentration of i) non complementary, ii) three base mismatch and iii) fully complementary target ssDNA are presented in Fig. 3. Percentage increase in charge transfer resistance was calculated using

$$\frac{R_{ct}^{HYB} - R_{ct}^{PROBE}}{R_{ct}^{PROBE}} \times 100 \quad (3)$$

$R_{ct}^{PROBE}$  is the charge transfer response of the probe before hybridisation and  $R_{ct}^{HYB}$  after hybridisation. The biosensor showed good selectivity as seen from the marked difference between the percentage  $R_{ct}$  increase of the complementary strands and the other two.

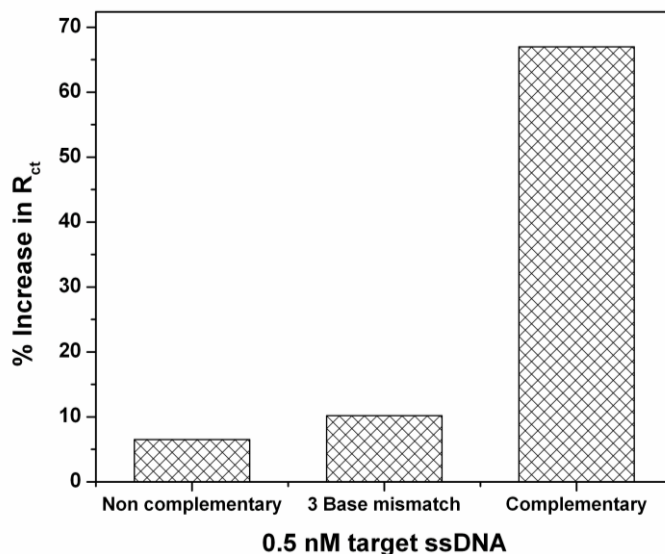


**Figure 3.** A bar chart showing the selectivity of the biosensor by comparing the response of GCE/G1PPI/ssDNA to different DNA targets sequences

#### 4. CONCLUSION

A simple DNA biosensor based on the application of dendrimer is developed. This work shows that the dendrimer – DNA compatibility, which is being exploited in the field of gene delivery, can be applied in the development of DNA biosensors. The rigorous chemistries and processes of electrode preparation and immobilisation have been simplified by the use of dendrimer. The biosensor stability is promising with remarkable detection limit and good selectivity. We have used this study as a proof of concept for the feasibility of DNA biosensors on dendrimer platform. It is envisaged that DNA biosensor for specific biomedical (or otherwise) application will stem from this work.

#### ACKNOWLEDGEMENT

The financial supports from the National Research Foundations (South Africa), the Claude Leon Foundations (South Africa), and Nanotechnology Innovation Centre, Mintek are gratefully acknowledged.

#### References

1. K.J. Odenthal and J.J. Gooding, *Analyst*, 132 (2007) 603
2. O.A. Arotiba, ELECTROCHEMICAL IMPEDANCE MODELLING OF THE REACTIVITIES OF DENDRIMERIC POLY(PROPYLENE IMINE) DNA NANOBIOSENSORS, in: Chemistry, University of the Western Cape, Bellville, 2008, pp. 247.

3. N.J. Ronkainen, H.B. Halsall and W.R. Heineman, *Chem. Soc. Rev.*, 39 (2010) 1747
4. K. Kerman, M. Kobayashi and E. Tamiya, *Measurement Science and Technology*, 15 (2004) R1
5. F. Lisdat and D. Schafer, *Analytical and Bioanalytical Chemistry*, 391 (2008) 1555
6. B. Pejčić and R. De Marco, *Electrochimica Acta*, 51 (2006) 6217
7. Osmotech, <http://www.osmetech.com/news/2006/pr290306.htm>
8. Warfarin, <http://www.medicalnewstoday.com/articles/115816.php>
9. W. Sun, P. Qin, H. Gao, G. Li and K. Jiao, *Biosensors and Bioelectronics* 25 (2010) 1264
10. H. Peng, C. Soeller and J. Travas-Sejdic, *Macromolecules*, 40 (2007) 909
11. P. Norouzi, M. Pirali-Hamedani, M. R. Ganjali and F. Faridbod, *International Journal of Electrochemical Science*, 5 (2010) 1434
12. A. Erdem, *Talanta*, 74 (2007) 318
13. J.M. Pingarrón, P. Yáñez-Sedeño and A. González-Cortés, *Electrochimica Acta*, 53 (2008) 5848
14. J. B. Raoof, M. S. Hejazi, R. Ojani and E. H. Asl, *International Journal of Electrochemical Science*, 4 (2009) 1436
15. A. Mohammadi, A. B. Moghaddam, R. Dinarvand and S. R. Zarchi, *International Journal of Electrochemical Science*, 4 (2009) 895
16. P. Du, H. Li, Z. Mei and S. Liu, *Bioelectrochemistry*, 75 (2009) 37
17. J.M. Fréchet, *Science*, 263 (1994) 1710
18. U. Boas, J.B. Christensen and P.M.H. Heegaard, *Journal of Materials Chemistry*, 16 (2006) 3785
19. C. Liang and M.J. Fréchet, *Prog. Polym. Sci.*, 30 (2005) 385
20. C. Dufes, I.F. Uchehgbu and A.G. Schatzlein, *Advanced Drug Delivery Reviews*, 57 (2005) 2177
21. T. Dutta, N.K. Jain, N.A.J. McMillan and H.S. Parekh, *Nanomedicine: Nanotechnology, Biology and Medicine*, 6 (2010) 25
22. S. Svenson and D.A. Tomalia, *Advanced Drug Delivery Reviews*, 57 (2005) 2106
23. G.R. Newkome and C.D. Shreiner, *Polymer*, 49 (2008) 1
24. A.-M. Caminade, C. Padié, R. Laurent, A. Maraval and J.-P. Majoral, *Sensors*, 6 (2006) 901
25. O.A. Arotiba, A. Ignaszak, R. Malgas, A. Al-Ahmed, P.G.L. Baker, S.F. Mapolie and E.I. Iwuoha, *Electrochimica Acta*, 53 (2007) 1689
26. O. Arotiba, J. Owino, E. Songa, N. Hendricks, T. Waryo, N. Jahed, P. Baker and E. Iwuoha, *Sensors*, 8 (2008) 6791
27. O.A. Arotiba, E.A. Songa, P.G. Baker and E.I. Iwuoha, *chimica oggi • Chemistry Today*, 27 (2009) 55
28. G. Li, X. Li, J. Wan and S. Zhang, *Biosensors and Bioelectronics*, 24 (2009) 3281
29. N. Zhu, H. Gao, Q. Xu, Y. Lin, L. Su and L. Mao, *Biosensors and Bioelectronics*, 25 (2010) 1498
30. O.A. Arotiba, J.H. Owino, P.G. Baker and E.I. Iwuoha, *Journal of Electroanalytical Chemistry*, 638 (2010) 287
31. W. Ehm, R. Kaus, C.A. Schiller and W. Strunz, New Trends in Electrochemical Impedance Spectroscopy and Electrochemical Noise Analysis, in: F. Mansfeld, F. Huet, O.R. Mattos (Eds.), vol. 2000-24, Electrochemical Society Inc, Pennington NJ, 2001, pp. 1.
32. P.M.S. Monk, *Fundamentals of Electroanalytical Chemistry*, Wiley, England, 2005
33. M.E. Orazem and B. Tribollet, *Electrochemical Impedance Spectroscopy*, in: John Wiley & Sons, Inc., New Jersey, (2008)
34. A. Bonanni, M.J. Esplandiú and M. del Valle, *Electrochimica Acta*, 53 (2008) 4022
35. J. Kafka, O. Pánke, B. Abendroth and F. Lisdat, *Electrochimica Acta*, 53 (2008) 7467
36. E. Katz and I. Willner, *Electroanalysis*, 15 (2003) 913